Biped Robot Reference Generation with Natural ZMP Trajectories

Okan Kurt and Kemalettin Erbatur
Faculty of Engineering and Natural Sciences, Sabanci University, Istanbul, Turkey
okankurt@su.sabanciuniv.edu erbatur@sabanciuniv.edu

Abstract— **Humanoid robotics attracted the attention of many researchers in the past 35 years. The motivation of research is the suitability of the biped structure for tasks in the human environment. The control of a biped humanoid is a challenging task due to the hard-to-stabilize dynamics.**

Walking reference trajectory generation is a key problem. A criterion used for the reference generation is that the reference trajectory should be suitable to be followed by the robot with its natural dynamics with minimal control intervention. Reference generation techniques with the so-called Linear Inverted Pendulum Model (LIPM) are based on this idea. The Zero Moment Point (ZMP) Criterion is widely employed in the stability analysis of biped robot walk. Improved versions of the LIPM based reference generation obtained by applying the ZMP Criterion are reported too. In these methods, the ZMP during a stepping motion is kept fixed in the middle of the supporting foot sole. This kind of reference generation lacks naturalness, in that, the ZMP in the human walk does not stay fixed, but it moves forward, under the supporting foot.

This paper proposes a reference generation algorithm based on the LIPM and moving support foot ZMP references. The application of Fourier series approximation simplifies the solution and it generates a smooth ZMP reference. Trajectory and force control methods for locomotion are devised and applied too. The developed techniques are tested through simulation with a 12 DOF biped robot model. The results obtained are promising for implementations.

I. INTRODUCTION

Humanoid robotics attracted the attention of many researchers in the past 35 years. It is currently one of the most exciting topics in the field of robotics and there are many projects on this topic [1-6]. The motivation of research is the suitability of the biped structure for tasks in the human environment and the goal of the studies in this area is to reach the human walking dexterity, efficiency, stability, effectiveness and flexibility.

The control of a biped humanoid is a challenging task due to the many degrees of freedom involved and the non-linear and hard to stabilize dynamics [7-8].

Walking reference trajectory generation is a key problem. Methods ranging from trial and error to the use of optimization techniques with energy or control effort minimization constraints are applied as solutions.

A very intuitive criterion used for the reference generation is that the reference trajectory should be suitable to be followed by the robot with its natural dynamics, without the use of extensive control intervention. Reference generation techniques with the so-called Linear Inverted Pendulum Model are based on this idea [9-10]. Simply stated, the walking cycle is then achieved by letting the robot start falling into the walking direction and to switch supporting legs to avoid the complete falling of the robot.

Yet another intuitive demand for the biped robot reference generation is that the reference trajectory should be a stable one, in the sense that it should not lead to unrecoverable falling motion. The Zero Moment Point Criterion [7] introduced to the robotics literature in early 1970s is widely employed in the stability analysis of biped robot walk. Improved versions of the Linear Inverted Pendulum Model based reference generation, obtained by applying the Zero Moment Point Criterion in the design process, are reported too [11]. In this approach the Zero Moment Point during a stepping motion is kept fixed in the middle of the supporting foot sole for the stability, while the robot center of mass is following the Linear Inverted Pendulum path.

Although reference generation with the Linear Inverted Pendulum Model and fixed Zero Moment Point reference positions is the technique employed for the most successful biped robots today, this kind of reference generation lacks naturalness at one point. Investigations revealed that the Zero Moment Point in the human walk does not stay fixed under the supporting foot. Rather, it moves forward from the heel to the toe direction [12-14].

In [14] Zhu et. al propose this idea of using variable ZMP to generate a dynamically stable gait in terms of linear inverted pendulum approach. They consider it to follow first order functions from the heel to toe of the foot in single support phase.

This paper takes a similar approach and proposes a reference generation technique based on the Linear Inverted Pendulum Model and moving support foot Zero Moment Point references. The application of Fourier series approximation to the solutions of the Linear Inverted Pendulum dynamics equations simplifies the solution as in [15], and it generates a smooth Zero Moment Point reference for the double support phase. Foot reference trajectory generation methods for smooth swing foot trajectories, trajectory control methods for the center of mass of the robot and force control techniques for the landing foot are employed in this paper too.

The reference generation and control techniques are simulated and animated in a 3-D full dynamics simulation

environment with a 12 DOF biped robot model. The results obtained are promising for implementations.

The biped model used as the test bed for the developed techniques is introduced in Section II. The reference generation with natural moving ZMP trajectories and the control of locomotion are discussed in Sections III and IV, respectively. Section V presents the simulation results and their analysis. The conclusion is drawn lastly.

II. The Biped Robot Model

The biped model used in this paper consists of two 6-DOF legs and a trunk connecting them (Fig. 1). Three joint axes are positioned at the hip. Two joints are at the ankle and one at the knee. Link sizes and the masses of the biped are given in Table I.

TABLE I
MASSES AND DIMENSIONS OF THE ROBOT LINKS

A. Link	**Dimensions (LxWxH) [m]**					**Mass [kg]**
Trunk	0.2	x	0.4	x	0.5	50
Thigh	0.27	x	0.1	x	0.1	12
Calf	0.22	x	0.05	x	0.1	0.5
Foot	0.25	x	0.12	x	0.1	5.5

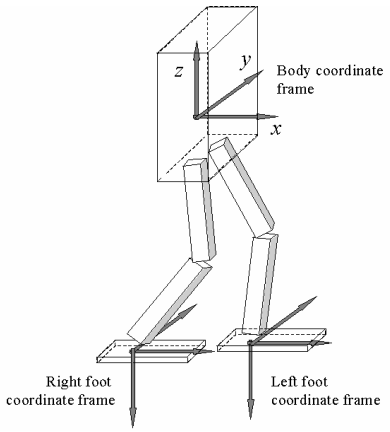

Figure 1. Biped robot coordinate frames.

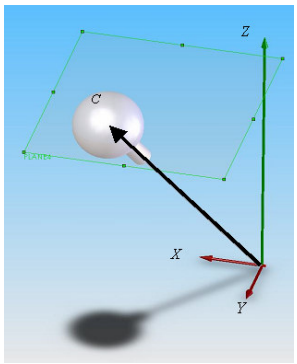

Figure 2. Inverted Pendulum.

III. Reference Generation with Natural ZMP Trajectories

LIPM mode approach is based on such ordinary differential equations that the solutions are both hard to be solved and they are composed of numerically unbounded *cosh(.)* functions. In addition they are sensitive to the height variation of the pendulum and they are difficult to be used robustly. Furthermore, since only the acceleration of the body is considered in LIPM approach the foot stepping positions may vary as a result. However, the stepping positions in real implementations are generally determined by exogenous environmental needs. For instance a robot should determine its foot stepping positions in order to avoid obstacles in real experiments. As a result the robot should have such a gait that follows the pre-determined stepping positions and preserve the overall stability. As a solution to such problems Choi, Y. et. al [15] introduce an alternative robust CoM trajectory planning method by using the approximate solution composed of bounded functions. Having pre-determined ZMP reference trajectories Choi, Y. et. al find the exact solutions of LIPM equations that are derived according to ZMP criterion. Finally they derive the approximated closed form equations that give the time trajectory of the CoM.

However in their studies Choi, Y. et. al use fixed ZMP trajectories. This actually leads the robot walking both to be rigid and unnatural. Furthermore, in their approximated solutions they do not consider double support phases which, eventually, may bring problems in real implementations. In this section an approximation to the solution of the dynamics of LIPM by considering natural ZMP references with double support phase is introduced.

A. Linear Inverted Pendulum Model

The main idea of the LIPM approach [9] is to extract a dominant feature of biped dynamics, which is high-order and non-linear, and to use this dominant factor to explain the governing dynamics of the system. In this model the robots mass is assumed to be lumped at the center of mass of the robot and the legs of the robot are assumed to be massless. Further, for simplicity, the height of the pendulum is assumed to be constant in this model. This lets the dynamics of the model to be linear. Such an inverted pendulum with a massless rod can be seen in Fig. 2 where $C = [c_x, c_y, c_z]^T$.

The ZMP equations for $x-y$ plane are as follows.

$$x_{zmp} = \frac{\sum_{i=1}^{n} m_i(\ddot{z}_i - g_z)x_i - \sum_{i=1}^{n} m_i(\ddot{x}_i - g_x)z_i}{\sum_{i=1}^{n} m_i(\ddot{z}_i - g_z)} \quad (1)$$

$$y_{zmp} = \frac{\sum_{i=1}^{n} m_i(\ddot{z}_i - g_z)y_i - \sum_{i=1}^{n} m_i(\ddot{y}_i - g_x)z_i}{\sum_{i=1}^{n} m_i(\ddot{z}_i - g_z)} \quad (2)$$

Let the ZMP of coordinates of this pendulum to be $P=\left[p_x, p_y, p_z\right]^T$, the mass of the pendulum to be m. The gravity vector is $g=\left[g_x, g_y, g_z\right]^T$ and $g_z=-g$. Using (1) and (2) the dynamics equations of the inverted pendulum can be derived as follows.

$$p_x=\frac{m\left(\ddot{c}_z+g\right)c_x-m\ddot{c}_x c_z}{m(\ddot{c}_z+g)} \tag{3}$$

$$p_y=\frac{m\left(\ddot{c}_z+g\right)c_y-m\ddot{c}_y c_z}{m(\ddot{c}_z+g)} \tag{4}$$

However (3) and (4) are non-linear. To attain linear equations the z-coordinate of the inverted pendulum is assumed to be constant. Let $c_z=z_c$. Thus the (3) and (4) turn into linear equations as follows.

$$p_x=c_x-\frac{1}{\omega_n^2}\ddot{c}_x \tag{5}$$

$$p_y=c_y-\frac{1}{\omega_n^2}\ddot{c}_y \tag{6}$$

where $\omega_n^2=\frac{g}{z_c}$. Henceforth, (5) and (6) are going to be referred as ZMP equations. Note that given the CoM coordinates of the pendulum $C=\left[c_x, c_y, c_z\right]^T$ at any time it is straightforward to calculate the ZMP coordinates of the pendulum by (5) and (6). On the other hand walking trajectory generation is the inverse problem, in that, given a ZMP trajectory a COM trajectory should be found [11]. Thus, this trajectory of COM could be used as a reference for the COM of the actual biped walking robot. Further the legs should be in such coordination that this COM is tracked accurately. Since the goal is to achieve a dynamically stable gait the ZMP trajectory should always lie inside the supporting polygon. And this actually determines the location of the footprints of the biped robot. Finally by knowing the footprints and the COM trajectory by inverse kinematics relations a possible gait could be achieved.

B. Natural ZMP Trajectories

The ZMP for a walking robot can either be measured by means of force sensors or it can be computed. The ZMP of the robot should be always in the supporting polygon for it to be in a stable condition. This implies that the robot is continuously recovering from unbalanced conditions to a stable posture. Stable ZMP references can be employed to design stable walking patterns.

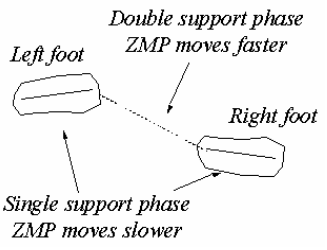

Figure 3. A Natural ZMP Trajectory.

Usually in many reported studies [11,15,16], the ZMP reference in the single foot support phase is in the form of a point under the sole of the supporting foot. However, experiments with walking humans show that the ZMP does not stay at a fixed point in the single support phase, [12-14]. It rather passes the sole of the supporting foot, from the heel to the toe.

A natural ZMP trajectory during the human walk cycle is illustrated in Fig. 3. We believe that using natural ZMP reference trajectories for gait generation will result in a more natural and energy efficient CoM trajectory. In fact, already reported results also show that -since the resulting CoM trajectory oscillations are smoother- using variable ZMP trajectories result in more energy efficient trajectories [14].

C. Exact Solution of LIPM for Fixed ZMP

Recall the ZMP equations (5) and (6). Rearranging these equations,

$$\ddot{c}_x=\omega_n^2 c_x-\omega_n^2 p_x \tag{7}$$

$$\ddot{c}_y=\omega_n^2 c_y-\omega_n^2 p_y \tag{8}$$

From the equations (7) and (8) applying Laplace transform,

$$C_x(s)=\frac{1}{1-\frac{1}{\omega_n^2}s^2}\left[p_x(s)-\frac{1}{\omega_n^2}C_x(0)s-\frac{1}{\omega_n^2}\dot{C}_x(0)\right] \tag{9}$$

$$C_y(s)=\frac{1}{1-\frac{1}{\omega_n^2}s^2}\left[p_y(s)-\frac{1}{\omega_n^2}C_y(0)s-\frac{1}{\omega_n^2}\dot{C}_y(0)\right] \tag{10}$$

In (9-10) the following fixed ZMP trajectories are going to be used for the exact solution calculation. In Fig. 4 the *x*-axis (for saggital plane) reference for ZMP trajectory, in Fig. 5 the *y*-axis (for frontal plane) reference for ZMP trajectory, and in Fig. 6 the resulting ZMP trajectory in the $x-y$ plane can be seen. Note that Fig. 5 also indicates the foot placement positions in the $x-y$ plane.

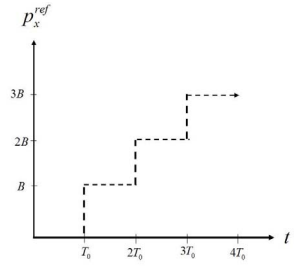

Figure 4. p_x^{ref}, x-axis ZMP reference trajectory.

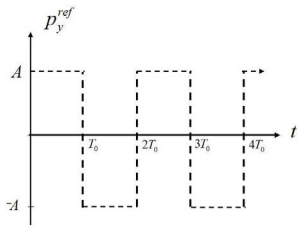

Figure 5. p_y^{ref}, y-axis ZMP reference Trajectory.

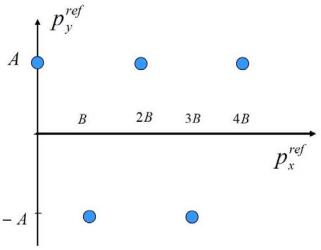

Figure 6. $p_y^{ref} - p_x^{ref}$ on $x-y$ plane ZMP ref. / Step Positions

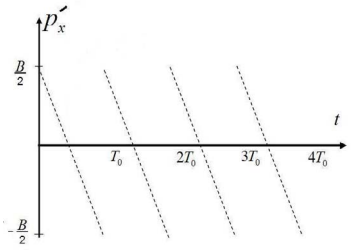

Figure 7. $p_x'(t)$ Introduced odd Function.

The ZMP reference trajectories in figures 4 and 5 can be expressed as follows.

$$p_x^{ref} = B\sum_{k=1}^{\infty} 1(t-kT_0) \tag{11}$$

$$p_y^{ref} = A1(t) + 2A\sum_{k=1}^{\infty}(-1)^K 1(t-kT_0) \tag{12}$$

Applying Laplace transform on these equations and substituting them in (9) and (10) with zero initial conditions, the following equations can be derived.

$$C_x(s) = \frac{1}{1-\frac{1}{\omega_n^2}s^2}\left[\frac{B}{s}e^{-T_0S} + \frac{B}{S}e^{-2T_0S} + \frac{B}{S}e^{-3T_0S} + \ldots\right] \tag{13}$$

$$C_y(s) = \frac{1}{1-\frac{1}{\omega_n^2}s^2}\left[\frac{A}{s} - \frac{2A}{s}e^{-T_0S} + \frac{2A}{S}e^{-2T_0S} - \frac{2A}{S}e^{-3T_0S} + \ldots\right] \tag{14}$$

With

$$\frac{1}{1-\frac{1}{\omega_n^2}s^2}\frac{1}{s} = \frac{1}{s} - \frac{s}{\left(s^2-\omega_n^2\right)},$$

(13) and (14) can be rearranged to derive the following functions.

$$\begin{aligned} C_x(s) &= B\left(\frac{1}{s} - \frac{s}{\left(s^2-\omega_n^2\right)}\right)e^{-T_0S} + B\left(\frac{1}{s} - \frac{s}{\left(s^2-\omega_n^2\right)}\right)e^{-2T_0S} \\ &\quad + B\left(\frac{1}{s} - \frac{s}{\left(s^2-\omega_n^2\right)}\right)e^{-3T_0S} + \ldots \end{aligned} \tag{15}$$

$$\begin{aligned} C_y(s) &= A\left(\frac{1}{s} - \frac{s}{\left(s^2-\omega_n^2\right)}\right) - 2A\left(\frac{1}{s} - \frac{s}{\left(s^2-\omega_n^2\right)}\right)e^{-T_0S} \\ &\quad + 2A\left(\frac{1}{s} - \frac{s}{\left(s^2-\omega_n^2\right)}\right)e^{-2T_0S} - \ldots \end{aligned} \tag{16}$$

Finally, we can obtain the exact reference trajectories of the CoM by applying inverse Laplace transformations to equations (15) and (16).

$$\begin{aligned} C_x(s) &= B(1-\cosh\omega_n(t-T_0))1(t-T_0) \\ &\quad + B(1-\cosh\omega_n(t-2T_0))1(t-2T_0) + \ldots \\ &= B\sum_{k=1}^{\infty}(1-\cosh\omega_n(t-kT_0))1(t-kT_0) \end{aligned} \tag{17}$$

$$\begin{aligned} C_y(s) &= A(1-\cosh\omega_n(t-T_0)) \\ &\quad - 2A(1-\cosh\omega_n(t-T_0))1(t-T_0) + \ldots \\ &= 2A\sum_{k=1}^{\infty}(-1)^k(1-\cosh\omega_n(t-kT_0))1(t-kT_0) \end{aligned} \tag{18}$$

Although (17) and (18) are the exact solutions for the ordinary differential equations (5) and (6), in practice they are difficult to be used robustly for a real biped walking robot since they are composed of numerically unbounded *cosh(.)* functions. Furthermore, they are unstable and very sensitive to the variation of ω_n. Therefore, an approximated solution composed of bounded *sin(.)* functions is suggested in [15] to serve as a robust CoM trajectory. This solution is outlined in the subsection below.

D. Planning an Approximate Solution

First an odd function with period T_0 is introduced from the *x*-directional reference ZMP p_x^{ref} of equation (5.11) as follows.

$$\begin{aligned} p_x'(t) &:= p_x^{ref}(t) - \frac{B}{T_0}\left(t - \frac{T_0}{2}\right) \\ &= \frac{B}{T_0}\left(t - \frac{T_0}{2}\right) \quad \text{and} \quad p_x'(t+T_0) = p_x'(t). \end{aligned} \tag{19}$$

Then assuming that the *x*-directional reference trajectory of CoM has the following form by using Fourier series,

$$C_x^{ref}(t) = \frac{B}{T_0}\left(t - \frac{T_0}{2}\right) + \sum_{n=1}^{\infty}\left[a_n\cos\left(\frac{n\pi}{T_0}t\right) + b_n\sin\left(\frac{n\pi}{T_0}t\right)\right] \tag{20}$$

Then applying the (20) to the ZMP differential equation (5) the following relation can be found.

$$p_x^{ref}(t) = \frac{B}{T_0}\left(t - \frac{T_0}{2}\right) + p_x'(t) \tag{21}$$

where

$$p_x'(t) = \sum_{n=1}^{\infty}\left[a_n\left(1+\frac{n^2\pi^2}{T_0^2\omega_n^2}\right)\cos\left(\frac{n\pi}{T_0}t\right) + b_n\left(1+\frac{n^2\pi^2}{T_0^2\omega_n^2}\right)\sin\left(\frac{n\pi}{T_0}t\right)\right] \tag{22}$$

Here in the equation (21) the form of the odd function $p_x'(t)$ can be seen in Fig. 7. Since $p_x'(t)$ is an odd function with period T_0, the coefficients $a_n = 0$ and b_n can be found by solving the following equation.

$$b_n\left(1+\frac{n^2\pi^2}{T_0^2\omega_n^2}\right) = \frac{2}{T_0}\int_0^{T_0} p_x'(t)\sin\left(\frac{n\pi}{T_0}t\right)dt \tag{23}$$

Finally b_n is found as

$$b_n = \frac{BT_0^2\omega_n^2(1+\cos n\pi)}{n\pi\left(T_0^2\omega_n^2 + n^2\pi^2\right)} \tag{24}$$

As a result, the *x*-directional reference trajectory of CoM can be obtained by substituting equation (24) to equation (20) as follows.

$$C_x^{ref}(t) = \frac{B}{T_0}\left(t - \frac{T_0}{2}\right) + \sum_{n=1}^{\infty}\left[\frac{BT_0^2\omega_n^2(1+\cos n\pi)}{n\pi\left(T_0^2\omega_n^2 + n^2\pi^2\right)}\sin\left(\frac{n\pi}{T_0}t\right)\right] \tag{25}$$

On the other hand, since the *y*-directional reference ZMP $p_y^{ref}(t)$ of the equation (12) is an odd function with

period T_0 the y-directional reference can be found in a similar manner as follows.

$$C_y^{ref}(t)=\sum_{n=1}^{\infty}\left[\frac{2AT_0^2\omega_n^2(1-\cos n\pi)}{n\pi\left(T_0^2\omega_n^2+n^2\pi^2\right)}\sin\left(\frac{n\pi}{T_0}t\right)\right] \tag{26}$$

The resulting CoM trajectories for x and y axes can be seen in Fig. 8. and from Fig. 9.

E. Introduction of Natural ZMP References by Fourier Approximation to Obtain CoM Trajectories

As discussed in the previous sections the ZMP trajectory in a human walking cycle is not fixed at a point at certain periods but it travels under the supporting polygon. In the single support phase the ZMP travels from heel to the toe of the foot and in the double support phase it travels from the toe of the supporting foot to the heel of the swinging foot [12-14]. In this context the x-directional reference ZMP trajectory p_x^{ref} is introduced as follows (Fig. 10). Here b is the half length of the foot sole. It can be observed that in this trajectory ZMP travel starts from zero and advances in time under the sole of the foot in the initial single support phase and from heel to the toe of the foot in the further single support phases. By the same procedure followed in the previous sections we introduce the following odd function p_x' with period T_0 from the x-directional reference ZMP p_x^{ref}, Fig. 11.

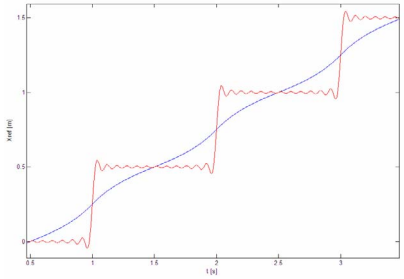

Figure 8. C_x Reference for x-axis (Saggital Plane, B=0.5, T_0 =1).

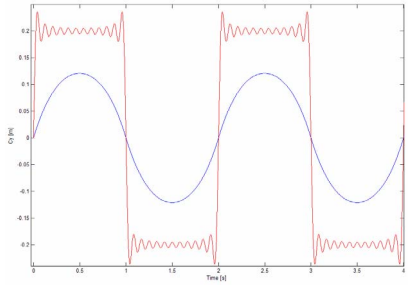

Figure 9. C_y Reference for y-axis (Frontal Plane, A=0.5).

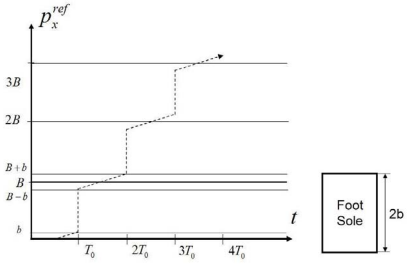

Figure 10. Natural ZMP Reference Trajectory

$$\begin{aligned} p_x'(t) &:= p_x^{ref}(t)-\frac{B}{T_0}\left(t-\frac{T_0}{2}\right) \\ &= \frac{B}{T_0}\left(t-\frac{T_0}{2}\right) \quad \text{and} \quad p_x'(t+T_0)=p_x'(t) \end{aligned} \tag{27}$$

Applying the same procedure from equation (19) to equation (23) we find the new b_n coefficient as follows.

$$b_n=\frac{(B-2b)T_0^2\omega_n^2(1+\cos n\pi)}{n\pi\left(T_0^2\omega_n^2+n^2\pi^2\right)} \tag{28}$$

Hence the natural CoM trajectory is found as

$$\begin{aligned} C_x^{ref}(t)=&\frac{B}{T_0}\left(t-\frac{T_0}{2}\right)+ \\ &\sum_{n=1}^{\infty}\left[\frac{(B-2b)T_0^2\omega_n^2(1+\cos n\pi)}{n\pi\left(T_0^2\omega_n^2+n^2\pi^2\right)}\sin\left(\frac{n\pi}{T_0}t\right)\right] \end{aligned} \tag{29}$$

The resulting C_x trajectory can be seen in Fig. 12. Note that this trajectory is smoother (shown in dashed line) than the conventional C_x trajectory (solid line) with fixed ZMP. The smoothness of the resulting trajectory implies that the acceleration differences are less when compared with the conventional C_x trajectory with fixed ZMP. This also implies that less energy is necessary to track the C_x trajectory with variable ZMP.

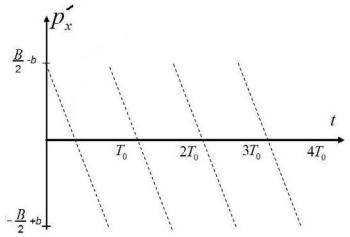

Figure 11. $p_x'(t)$ New introduced odd function.

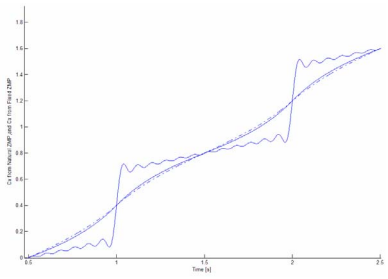

Figure 12. C_x Trajectory with Variable ZMP.

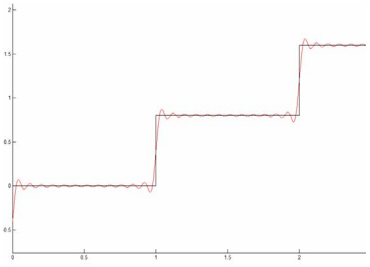

Figure 13. Fourier Approximation w/o Lanczos Sigma Factor

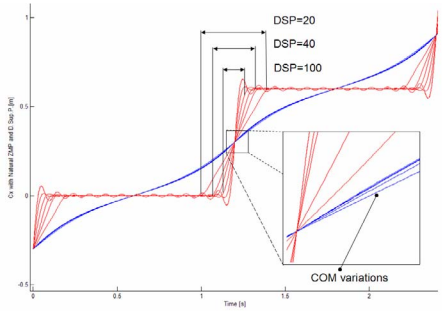

Figure 14. Fourier Approximation with Lanczos Sigma Factor

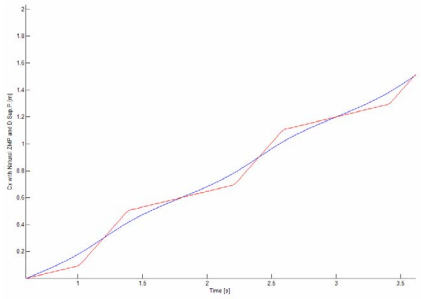

Figure 15. Natural C_X reference with parameters close to human walk

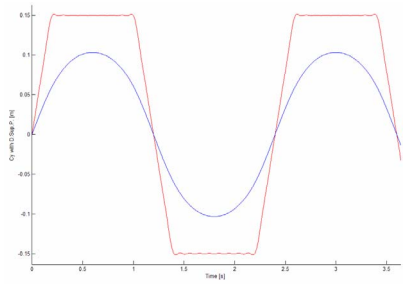

Figure 16. Natural C_Y reference with parameters close to human walk

F. Introducing Double Support Phase to ZMP References

In this section the introduction of double support phases to previously used reference ZMP trajectories will be addressed. Adding double support phase to reference ZMP trajectories in both *x* and *y* axes by the method above, which is to blend lines with different slopes, makes it impossible to overcome such a problem. Instead to overcome this problem the so-called Lanczos Sigma Factor is used for such a task.

The non-uniform convergence of the Fourier series for discontinuous functions is known as Gibbs Phenomenon in the literature. There are complex methods to smooth the Gibbs Phenomenon. One method is the so-called Lanczos Sigma Factor. In this approximation a function is multiplied by the coefficients in the Fourier partial sums. This function is a complex *sine* function involving the period of the original function. Fourier series by the Lanczos Sigma Factor can be rewritten as follows.

$$f(\theta)=\frac{a_0}{2}+\sum_{n=1}^{m-1}\sin c(\frac{n\pi}{m})\left[a_n\cos(n\theta)+b_n\sin(n\theta)\right] \tag{30}$$

The resulting effect of the Lanczos Sigma Factor can be seen in Fig. 13 and Fig. 14.

In this example the Double Support Parameter DSP of the Lanczos Sigma Factor ($\sin c(\frac{n\pi}{DSP})$) is used to attain double support phases in the reference ZMP trajectory. Notice that in Fig. 14. the duration of the double support phase is tuned by setting appropriate values to the DSP parameter. Also observe the variations of the CoM trajectory corresponding to different double support phase durations. Further the found Natural CoM trajectories for $x-y$ axes are as follows.

$$C_x^{ref}(t)=\frac{B}{T_0}\left(t-\frac{T_0}{2}\right)+\sum_{n=1}^{\infty}\left[(B-2b)\frac{BT_0^2\omega_n^2(1+\cos n\pi)}{n\pi(T_0^2\omega_n^2+n^2\pi^2)}\sin c\left(\frac{n\pi}{DSP}\right)\sin\left(\frac{n\pi}{T_0}t\right)\right] \tag{31}$$

$$C_y^{ref}(t)=\sum_{n=1}^{\infty}\left[\frac{2AT_0^2\omega_n^2(1-\cos n\pi)}{n\pi(T_0^2\omega_n^2+n^2\pi^2)}\sin c\left(\frac{n\pi}{DSP}\right)\sin\left(\frac{n\pi}{T_0}t\right)\right] \tag{32}$$

In addition the Natural ZMP trajectories for $x-y$ axes are obtained by

$$p_{xNatural}^{ref}(t)=\frac{B}{T_0}\left(t-\frac{T_0}{2}\right)+\sum_{n=1}^{\infty}\left[\frac{(B-2b)(1+\cos n\pi)}{n\pi}\sin c\left(\frac{n\pi}{DSP}\right)\sin\left(\frac{n\pi}{T_0}t\right)\right] \tag{33}$$

$$p_{yNatural}^{ref}(t)=\sum_{n=1}^{\infty}\left[\frac{2A(1-\cos n\pi)}{n\pi}\sin c\left(\frac{n\pi}{DSP}\right)\sin\left(\frac{n\pi}{T_0}t\right)\right] \tag{34}$$

As an example, trajectory for the walking parameters close to a human's is given in Fig. 15, and in Fig. 16. (A=.15[m], B=.6[m], b=[.14] and T_0 =1 [s])

IV. Outline of The Control Algorithm

The swing foot position references are obtained from ZMP and CoM references (Fig. 17). The control algorithm consists of five lower level position and force controller building blocks (Fig. 18). Swing foot references, or alternatively, the swing timing determines the timing for switching between control structures. However, swing reference timing is not the only criterion to switch from one control mode to the other. Switching from swing to support controller before actually reaching the ground level and establishing stable contact with the ground can cause a sudden loss of the robot balance. Therefore, ground interaction force information is used and controller mode switching is not allowed before the z-direction component of the contact force exceeds a certain threshold value. The force threshold value is a design parameter. The support-to-swing switching times are according to the swing timing without additional feedback from ground interaction forces. The double

support controller regards the biped robot as a trunk manipulated by two six-DOF arms with their bases positioned on the ground level (Fig. 19, left). The CoM position reference discussed above and fixed orientation reference with respect to the world coordinate frame are applied in a position control schemes for both manipulators. The position controllers running for the two manipulators (legs) are identical. Cartesian position and orientation errors are computed from the reference and actual position and orientations. These errors are reflected to the joint space errors by the use of inverse Jacobian relations. Independent joint PID controllers are employed for the joint space position control. The controllers for the two legs work almost independently. However, the Cartesian errors are scaled with different gains for the two legs before corresponding joint errors are computed. The scaling factor for the right leg is proportional to the horizontal distance of the left foot coordinate center from the CoM and similarly, the scaling factor for the left leg is proportional to the horizontal distance of the right foot from the CoM. This rule is obtained experimentally and it performed well for the coordination of the two legs in the double support phase. The robot in swing phases can be seen as a ground based manipulator controlling the CoM position and trunk orientation and a second manipulator based at the hip controlling the swing foot position and orientation. The right support and left swing controllers are activated simultaneously. The single support controller applies the position control scheme described above for the double support phase (without using the scaling factors). The swing leg controller is a stiffness controller for the foot position and orientation. For soft landing purposes, a Cartesian stiffness matrix with low stiffness against in orientation errors and position errors in the z-direction is employed. The horizontal directions are penalized with higher stiffness coefficients.

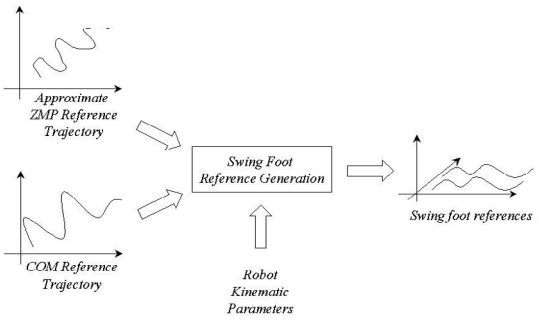

Figure 17.The swing foot references are obtained from ZMP and CoM references.

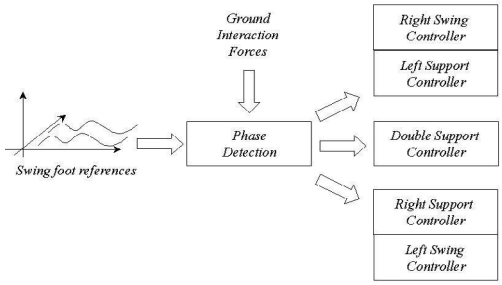

Figure 18.The swing foot position references are obtained from ZMP and CoM references.

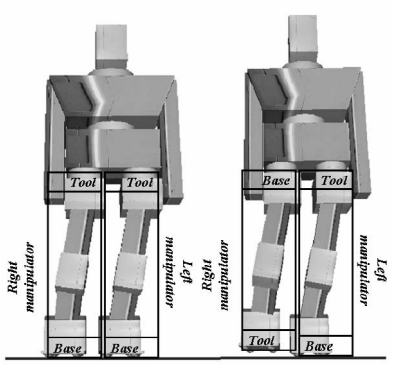

Figure 19. The robot in the double support phase can be regarded as a trunk manipulated by two six-DOF manipulators based on the ground (left). The robot in swing phases can be seen as a ground based manipulator and a second manipulator based at the hip (right).

V. SIMULATION RESULTS

Simulations studies are carried out with the robot model described in Section II, references generated in Section III and the coordination and control mechanism discussed in Section IV. The simulation scheme is similar to the one in [17]. The details of the algorithm and contact modeling can be found in [18]. Parameters used for reference generation are presented in Table II. Fig. 20 shows the y-direction CoM and CoM reference. It can be observed that the COM reference in this direction is closely tracked except in the single support phases. The y-direction ZMP and ZMP reference curves displayed in Fig. 21 also a deviation from the reference curve in the swing phases. This suggests that the simple LIMP model, concentrating on the robot trunk, and ignoring the effects of the swing foot on the CoM of the whole robot, may encounter problems when the leg weight is not very low. The legs weigh 15 kg. Although it is much less than the 50 kg trunk weight, this weight affects the y-direction COM and ZMP curves significantly. Apart from the swing phases, the tracking performance is quite acceptable. The x-direction COM and ZMP curves together with their references are presented in figures 22 and 23, respectively. These curves, too, display oscillations and deviations from reference curves mainly due to the trunk dominated LIMP model. Still, in the average, the reference curves are tracked.

TABLE II
Some of the important simulation parameters

Parameter	*Value*
x-reference foot-CoM offset	-0.11 m
Step height	0.02 m
Step period	3 s
Foot to foot y-direction distance	0.08 m
Foot to foot y-direction ZMP reference distance	0.1 m
Ground interaction threshold force	100 N

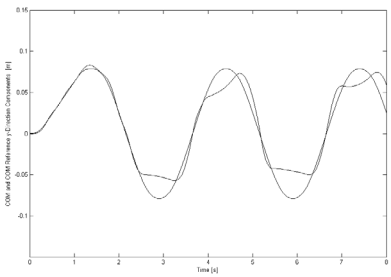

Figure 20. CoM and CoM reference *y*-direction components.

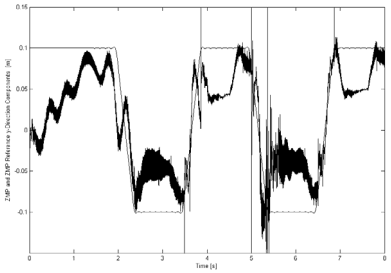

Figure 21. ZMP and ZMP reference *y*-direction components

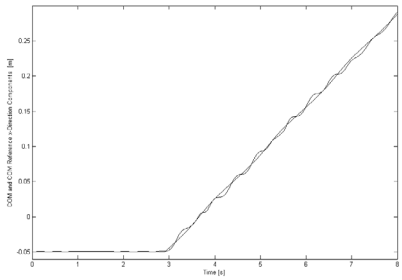

Figure 22. CoM and CoM reference *x*-direction components

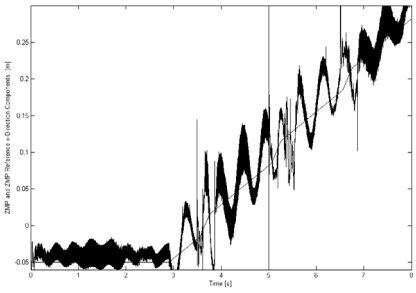

Figure 23. ZMP and ZMP reference *y*-direction components

In the average, the ZMP curve moves forward even in the single support phases. However, the transient behavior does not indicate that the naturalness of the human walk is achieved completely. Although there are some tracking problems as discussed above, the reference generation and control algorithms are generally successful, keeping the ZMP in the support polygon and enabling the robot move forward with an almost constant speed of 7 cm per second. This is achieved without the need for the elaborate trial and error steps common to many other reference generation approaches.

VI. CONCLUSION

A trajectory generation, coordination and control approach for biped walking robots is presented in this paper. Human-like ZMP reference trajectories with Fourier series approximation techniques for the solution of LIPM dynamics equations are employed in order to achieve naturalness in the walk. A control structure consisting of different modes and position and force control techniques is employed. Simulation studies show that the reference generation without considering the effects of the swing foot on robot ZMP can lead to significant deviations from reference trajectories. The walk, however, is stable and this is promising result making the algorithm a candidate for implementation.

REFERENCES

[1] Sakagami, Y., Watanabe, R., Aoyama, C., Shinichi, M., Higaki, N., Fujimura, K., "The intelligent ASIMO: System overview and integration", *Proceedings of the IEEE International Conference on Intelligent Robots and Systems*, Lausanne, Switzerland, October 2002

[2] Sawada, T., Takagi, T. and Fujita, M., "Behavior Selection and Motion Modulation in Emotionally Grounded Architecture for QRIO SDR-4X II", *Proceedings of the IEEE International Conference on Intelligent Robots and Systems, vol.3, pp. 2514-2519*, Sendal, Japan, October 2004.

[3] Lohmeier, S., Löffler, K., Gienger, M., Ulbrich, H., Pfeiffer, F., "Computer System and Control of Biped "Johnnie"", *Proceedings of the IEEE International Conference on Robotics and Automation, vol.4, pp.4222-4227*, New Orleans, LA, April 2004.

[4] Kaneko, K., Kanehiro, F., Kajita, S., Yokoyama, K., Akachi,K., Kawasaki, T., Ota, S., Isozumi, T., "Design of Prototype Humanoid Robotics Platform for HRP", *IEEE International Conference on Intelligent Robots and Systems, pp.2431-2436, vol.3*, October 2002.

[5] www.humanoid.waseda.ac.jp/booklet/kato02.html

[6] Hirai, K., M. Hirose, Y. Haikawa, T. Takenaka, "The Development of Honda Humanoid Robot", *Proceedings of IEEE International Conference on Robotics and Automation, pp: 1321 - 1326 vol.2*, May 1998

[7] Vukobratovic, M., Borovac, B., Surla, D. and Stokic, *Biped Locomotion: Dynamics, Stability and Application*. Springer-Verlag, 1990.

[8] Marc Raibert, *Legged Robots that Balance*, MIT Press, Cambridge, MA, 1986.

[9] Kajita, S., Tani, K. "Study of Dynamic Biped Locomotion on Rugged Terrain –Theory and Basic Experiment-" *ICAR, Fifth International Conference on Advanced Robotics, pp: 741-746, vol.1*, June 1991.

[10] Kajita, S., Kaehiro, K., Kaneko, K., Fujiwara, K., Yokoi, K., Hirukawa, H.," A Real Time Pattern Generator for Bipedal Walking" *Proceedings of the IEEE International Conference on Robotics and Automation, vol.1, pp.31-37*, May 2002.

[11] Kajita, S., Kahehiro, F., Kaneko, K., Fujiwara, K., Harada, K., Yokoi, K., Hirukawa, H., " Biped Walking Pattern Generation using Preview Control of the Zero-Moment-Point", *Proceedings of IEEE International Conference on Robotics and Automation, pp: 1620 - 1626, vol.2*, Taipei, Taiwan, September 2003.

[12] Dasgupta, A., Nakamura, Y. "Making Feasible Walking Motion of Humanoid Robots from Human Motion Capture Data" *Proceedings of the IEEE International Conference on Robotics and Automation*, Detroit, Michigan, May 1999.

[13] Erbatur, K., A. Okazaki, K. Obiya, T. Takahashi and A. Kawamura, "A Study on the Zero Moment Point Measurement for Biped Walking Robots", *Proc. 7th International Workshop on Advanced Motion Control, pp. 431-436*, Maribor, Slovenia, 2002

[14] Zhu, C., Tomizawa, Y., Luo, X., Kawamura, A. "Biped Walking with Variable ZMP, Frictional Constraint, and Inverted Pendulum Model", *IEEE International Conference on Robotics and Biomimetics, pp: 425 – 430*, Shenyang, China Aug 2004.

[15] Choi, Y., You, B.J., Oh, S.R., "On the Stability of Indirect ZMP Controller for Biped Robot Systems", *Proceedings of International Conferenc on Intelligent Robots and Systems, pp: 1966 - 1971, vol.2*, Sendal, Japan, June 2004.

[16] Sugihara, T., Nakamura, Y., Inoue, H., "Real-time Humanoid Motion Generation Through ZMP Manipulation based on Inverted Pendulum Control", *Proceedings of IEEE International Conference on Robotics and Automation, pp: 1404 - 1409, vol.2*, Washington DC, May 2002.

[17] Fujimoto, Y., A. Kawamura, "Simulation of an Autonomous Biped Walking Robot Including Environmental Force Interaction", *IEEE Robotics and Automation Magazine, pp. 33-42,* June 1998.

[18] Erbatur, K. and A. Kawamura, "A New Penalty Based Contact Modeling and Dynamics Simulation Method as Applied to Biped Walking Robots," *Proc. 2003 FIRA World Congress*, October 1-3, 2003 Vienna, Austria